Geophys. J. Int. (2002) **150,** 37–44

A reappraisal of regional surface wave tomography

B. L. N. Kennett and K. Yoshizawa

Research School of Earth Sciences, Australian National University, Canberra ACT 0200, *Australia. E-mail: brian@rses.anu.edu.au*

Accepted 2001 December 12. Received 2001 December 10; in original form 2001 March 26

SUMMARY

A three-stage inversion scheme for surface wave tomography working with multimode phase dispersion as a function of frequency provides a means of combining a wide range of data in a common framework. The phase average approximation is applied directly to phase slowness and there is no need to invoke perturbation arguments for the interpretation of path-averaged velocity models derived from waveform inversion of surface waves. By treating such wave speed profiles as summaries of path specific dispersion behaviour it is possible not only to combine results from different style of inversion but also to provide maximum exploitation of Love and Rayleigh wave information. Inversions of all suitable waveforms can be undertaken in terms of isotropic models. Dispersion information from all paths is combined to form multimode phase speed distributions as a function of frequency in linearized inversion which takes account of path bending and finite frequency effects. The final inversion for 3-D wave speed structure is based on a cellular inversion of the multimode frequency dispersion including angular effects in terms of a local stratified model including anisotropy. The smoothing from inclusion of finite frequency effects and damping of the linearized inversion for the phase speed distributions will control the smoothness of the 3-D shear wave speed model.

Key words: dispersion, multimode analysis, surface wave tomography, waveform inversion.

1 INTRODUCTION

Current approaches to surface wave tomography on a regional scale are based either on the exploitation of fundamental mode dispersion (Ritzwoller & Levshin 1998) or on the use of multimode synthetics to match waveforms on individual paths (based on the work of Nolet 1990). In the partitioned waveform approach formalised by Nolet (1990), the 1-D models obtained by waveform fitting are interpreted as the average structure along the path between source and receiver. The ensemble of path averaged constraints are then used in a linear inversion to recover 3-D structure (Zielhuis & Nolet 1994). The waveform inversion is based on linearized inversion with either direct use of the seismograms (Nolet *et al.* 1986) or the use of secondary variables based on cross-correlation between observed and synthetic seismograms (Cara & Lévêque 1987). Both methods show dependence on the reference model used for initiating the inversion. The domain of quasi-linear behaviour is larger with the use of secondary variables, so that a single mantle reference model has been employed for a large number of paths (Debayle & Kennett 2000a). The second stage linear inversion can be constructed as a form of cellular tomography (Zielhuis & Nolet 1994), or in a continuous representation with an imposed Gaussian smoothing, defined by a model cross-correlation length based on the continuous regionalisation scheme of Montagner (1986).

The common feature of all the different applications is that the models obtained in the first stage of the process are interpreted directly as averages along the paths. It has been pointed out by Marquering *et al.* (1996) that, as frequency increases, this path-average assumption has significant limitations for higher mode information representing body waves, since the sensitivity of the data is concentrated around the body wave paths. Improved results for data set with a large higher mode component can be obtained, at considerable computational cost, by incorporating an allowance for coupling between the modes for the reference structure. The inversion procedure is then both iterative and non-linear.

The more common approach has been to enlarge the size of the data set so that dense path coverage is brought to bear on the delineation of structure. For example, for the Australian region, Simons *et al.* (1999) and Debayle & Kennett (2000a) have used more than two thousand paths in inversions using Rayleigh waves. With such path densities, it is possible to extend the second stage inversion to try to extract angular dependence from the path averages and so attempt to define azimuthal anisotropy (Debayle & Kennett 2000a).

Much regional surface wave tomography has been carried out using just Rayleigh waves recorded on the vertical component. However, Lévêque *et al.* (1998) used both Rayleigh and Love wave data for a limited number of paths across the Indian Ocean region, with a model of transverse isotropy with a vertical symmetry axis (TIV) for each path. From the set of 1-D models for the paths both wave speed variations and anisotropic components were extracted, revealing azimuthal and polarization effects (Lévêque *et al.* 1998). This approach was extended to a much larger data set for the Australian region by Debayle & Kennett (2000b) and used to demonstrate the presence of significant polarization anisotropy between

vertical and horizontal *S* wave propagation. The pattern of polarization anisotropy shows significant lateral variation and does not have a direct association with the wave speed patterns revealed by earlier inversion based on Rayleigh waves alone. With the use of TIV models both Rayleigh and Love wave observations are needed for each source-station pair, which limits the available paths.

In this paper we reappraise the way in which we can exploit multimode surface wave information for regional tomography, particularly in the context of anisotropic inversion. The levels of heterogeneity revealed in recent studies of the upper mantle are too high for the path-average assumption to be applied directly to the 1-D model representing a fit to the observed seismograms. However, for the frequency interval in which modal interaction can be neglected, we can use the path-average assumption for individual mode contributions and regard the 1-D model as a representation of the character of multimode dispersion along the source-receiver path. This viewpoint is reinforced by investigation of fully non-linear inversion for surface wavetrains (Yoshizawa & Kennett 2002a) which demonstrates the possibility of extracting different styles of 1-D models with a comparable fit to data. Although the models differ significantly, the dispersion of the first few modes over the frequency range controlled by the data cannot be distinguished.

We will show that the procedure for regional surface-wave tomography can be reformulated as a three-stage process working with multimode dispersion (rather than the two steps of the partitioned waveform inversion approach). The stages are construction of path information by waveform fitting, building multimode phase-speed maps as a function of frequency and then a final inversion for local wave speed properties.

The new scheme offers the advantage of allowing the incorporation of different style of information such as dispersion measurements, angles of incidence and waveform constraints within a single formulation. By working directly with phase speed we can incorporate the deviation of paths from the great-circle using ray tracing for individual modes and take account of the extended influence zone around each ray path (Yoshizawa & Kennett 2002b).

2 PATH-AVERAGE APPROXIMATIONS

The basis for the use of the path-average approximation comes from the analysis of Woodhouse (1974) for surface wave propagation in a quasi-stratified medium with slowly varying seismic properties. In a high-frequency approximation the passage of an individual surface-wave mode can be described by a ray theory, where the trajectory is controlled by the phase-speed variations in the model. The local phase speed for the mode is determined by the dispersion characteristics of the stratified structure in the column beneath the point of interest. The accumulated phase along the path is the integral of the local phase slowness p; thus for the jth mode, at angular frequency ω, the phase contribution is

$$\omega\phi_j(\omega) = \omega \int_{\mathrm{ray}_j} ds\; p_j(s,\omega), \tag{1}$$

where the integration of the local slowness $p_j(s,\omega)$ is taken along the ray path for the mode. For a epicentral distance X we can then extract an average slowness $\langle p_j(\omega)\rangle$ for the jth mode from

$$\phi_j(\omega) = X\langle p_j(\omega)\rangle. \tag{2}$$

When the ray path departs from the great-circle between source and receiver $\langle p_j(\omega)\rangle$ will be overestimated, because X will be shorter than the true path length.

The leading order term in the asymptotic approximation involves only the jth mode, whereas the higher order corrections can be written in a form which includes cross-mode coupling along the ray path for the jth mode.

The path-average approximation will breakdown in the presence of rapid changes in seismic parameters compared to the wavelengths of the surface waves. Such strong heterogeneity is likely to produce significant deviations of the surface wave path from the great circle between source and receiver, with induced coupling between modal contributions. The problems are most severe at higher frequencies as the wavelength shortens, and for the higher modes which sum to represent body-wave contributions. Marquering *et al.* (1996) show that a limited allowance for mode-coupling along the path can provide an improved treatment of intermediate-period body waves by providing concentration of sensitivity around the body-wave ray path, rather than spread along the whole segment as in the path-average approximation.

2.1 Representation of surface wave seismograms

To the leading-order asymptotic approximation, the contribution to the surface wave portion of the seismogram from a number of modes can be written as

$$u(X,\omega) = \sum_{j=0}^{J} \mathcal{R}_j(X,\omega) \exp\left\{ \mathrm{i}\omega \int_{\mathrm{ray}_j} ds\; p_j(s,\omega) \right\} \mathcal{S}_j(\omega), \tag{3}$$

in the far-field of the source. $\mathcal{S}_j(\omega)$ represents the excitation imposed by the source through terms dependent on the source depth. $\mathcal{R}_j(X,\omega)$ includes the terms dependent on receiver depth and the geometric spreading of the surface waves. We can account for surface wave attenuation by allowing the local phase slowness p_j to be complex. For a laterally varying medium $\mathcal{S}_j$, $\mathcal{R}_j$ are usually evaluated using the structures appropriate to the source and receiver positions. But, as pointed out by Kennett (1995), these contributions are not localised and include some path dependency. If we make the replacement of the cumulative phase speed contribution (1) by the equivalent averaged phase term (2), for each mode, we can rewrite the seismogram representation (3) as

$$u(X,\omega) = \sum_{j=0}^{J} \mathcal{R}_j(X,\omega) \exp\{\mathrm{i}\omega X\langle p_j(\omega)\rangle\} \mathcal{S}_j(\omega), \tag{4}$$

the form expected for a stratified medium for which the dispersion of the jth mode was described by $\langle p_j(\omega)\rangle$. It is this equivalence that is exploited in inversion of the waveforms of surface waves in terms of a path-specific stratified model.

2.2 Path-averaged models?

The basis of the two stage inversion for 3-D shear wave speed structure in the Partitioned Waveform Inversion (PWI) scheme of Nolet (1990) is that the stratified model obtained by fitting observed waveforms represents the average of the shear wave speed along the great-circle path from source to receiver. As we shall see, this is a reasonable approximation if the variations in seismic structure encountered along the path are sufficiently small that first-order perturbation theory can be applied. However, there are now indications of contrasts in crustal and mantle structures which are strong enough to lie outside the domain of linearized analysis. Examples include the edge of a shield, e.g. Simons *et al.* (1999) and Debayle & Kennett

(2000a) in studies of Australia, and a direct transition from oceanic to continental structure.

We introduce a stratified model of shear wave speed $\beta^0(z)$, as a function of depth z, for which we can calculate an approximation to the observed seismogram,

$$u^0(X,\omega) = \sum_{j=0}^{J} \mathcal{R}_j^0(X,\omega) \exp\{\mathrm{i}\omega X p_j^0(\omega)\}\, \mathcal{S}_j^0(\omega), \tag{5}$$

based on a suitable representation of source excitation. The effects of attenuation can be included through using a complex wave speed at each frequency to calculate the mode slownesses $p_j^0(\omega)$.

We then look to improve the representation of the observed seismogram by modifying the shear wave speed distribution; the effect of density is commonly either ignored or linked to wave speed variation by some scaling. If the excitation terms are adequately described, the dominant contribution to the surface wave seismogram will come from the modal phase terms. Thus, using the leading-order asymptotic representation (3) to represent the observations, we can recast the exponential term and extract the contribution for the reference model $\beta^0(z)$:

$$\begin{aligned} u(X,\omega) &= \sum_{j=0}^{J} \mathcal{R}_j(X,\omega) \exp\left\{ \mathrm{i}\omega X p_j^0(\omega) \right. \\ &\qquad \left. + \mathrm{i}\omega \left[\int_{\mathrm{ray}_j} ds\, \{p_j(s,\omega)\} - X p_j^0(\omega) \right] \right\} \mathcal{S}_j(\omega), \\ &= \sum_{j=0}^{J} \mathcal{R}_j(X,\omega) \exp\{\mathrm{i}\omega X p_j^0(\omega) + \mathrm{i}\omega \delta\phi_j\}\, \mathcal{S}_j(\omega), \end{aligned} \tag{6}$$

The phase perturbation $\omega\delta\phi_j(\omega)$ between the actual and reference media can be expressed through

$$\delta\phi_j = \int_{\mathrm{ray}_j} ds\{p_j(s,\omega)\} - X p_j^0(\omega) = \int_0^X ds\, \left\{ \hat{p}_j(s,\omega) - p_j^0(\omega) \right\}, \tag{7}$$

in terms of the projected slowness $\hat{p}_j$ along the great-circle between source and receiver. With the restriction to just variations in shear wave speed $\delta\beta(z,s)$ from the reference mode $\beta^0(z)$ along the path,

$$\begin{aligned} \hat{p}_j(s,\omega) - p_j^0(\omega) = \int_0^{\mathrm{a}} dz \left[\frac{\partial \hat{p}_j}{\partial \beta(z,s)} \delta\beta(z,s) \right. \\ \left. + \frac{\partial^2 \hat{p}_j}{\partial \beta^2(z,s)} [\delta\beta(z,s)]^2 + \cdots \right], \end{aligned} \tag{8}$$

where a is the radius of the Earth. To a first order approximation, the perturbation

$$\delta\phi_j = \int_0^X ds \int_0^{\mathrm{a}} dz \frac{\partial \hat{p}_j}{\partial \beta(z,s)} \delta\beta(z,s), \tag{9}$$

and with a change in the order of integration

$$\delta\phi_j = \int_0^{\mathrm{a}} dz \int_0^X ds \frac{\partial \hat{p}_j}{\partial \beta(z,s)} \delta\beta(z,s). \tag{10}$$

Now introduce the average perturbation in shear structure along the path at each depth,

$$\langle \delta\beta(z) \rangle = \frac{1}{X} \int_0^X ds\, \delta\beta(z,s), \tag{11}$$

and make a linearized treatment about this path-averaged model; then

$$\begin{aligned} \delta\phi_j = \int_0^{\mathrm{a}} dz \int_0^X ds \left(\left. \frac{\partial \hat{p}_j}{\partial \beta(z)} \right|_{\beta^0 + \langle \delta\beta \rangle} + \left. \frac{\partial^2 \hat{p}_j}{\partial \beta^2(z)} \right| \bar{\Delta}\beta(z,s) \right) \\ \times (\langle \delta\beta(z) \rangle + \bar{\Delta}\beta(z,s)), \end{aligned} \tag{12}$$

where we have written $\bar{\Delta}\beta(z,s) = \delta\beta(z,s) - \langle \delta\beta(z) \rangle$. When we recognise that

$$\int_0^X ds\, \bar{\Delta}\beta(z,s) \equiv 0,$$

we see that

$$\begin{aligned} \delta\phi_j = \int_0^{\mathrm{a}} dz\, \langle \delta\beta(z) \rangle \left. \frac{\partial \hat{p}_j}{\partial \beta(z)} \right|_{\beta^0 + \langle \delta\beta \rangle} \\ + \int_0^{\mathrm{a}} dz \left. \frac{\partial^2 \hat{p}_j}{\partial \beta^2(z)} \right| \int_0^X ds\, [\bar{\Delta}\beta(z,s)]^2. \end{aligned} \tag{13}$$

The first term corresponds to a stratified model with the path averaged structure $\beta^0(z) + \langle \delta\beta(z) \rangle$. The correction term depends on the square of the deviations of the actual structure from the path average and will become important if there are significant portions of the path with more than about 4 per cent deviation from the path-averaged structure.

If the variations in the true seismic structure along the path are small, it is a reasonable approximation to assume that a waveform inversion in terms of a stratified model will yield a path-averaged model. We note that this is quite a strong requirement; it is not just the shift associated with the path-average model that is required to be small but also the true deviations from the model.

Even in circumstances where the path-average model assumption is inadequate the representation of the seismogram in terms of the cumulated phase contributions from each of the modes (1) can be made, although the paths for the individual modes may be different. The assumption of independent mode propagation, which underlies this treatment, depends only on slow variations in wave speed and not on the actual differences from the reference model.

The propagation of surface waves in 3-D models can be simulated using direct numerical methods or via mode and wavenumber coupling (Kennett 1998). However, numerical implementations for the relatively long paths (in terms of wavelengths) needed for simulating regional tomography are not yet available. Testing of waveform inversion procedures has therefore been confined so far to stratified models.

An extensive set of synthetic tests for stratified media (Hiyoshi 2001) shows that a direct linearized inversion procedure (Nolet *et al.* 1986) will provide good recovery of the true model for perturbations in velocity of the order of ±2 per cent. This makes the choice of starting model $\beta^0(z)$ critical to the success of this class of waveform inversion.

By employing secondary variables, as in the work of Cara & Lévêque (1987), the domain of practical inversion for stratified models for Rayleigh wave observations can be expanded to ±8 per cent deviations from the reference model. However, the limitations on the interpretation of the recovered model remain. Only for small shifts from the reference model can the model obtained by waveform inversion of observed data be regarded as an average of the shear wave speed structure encountered along the path. For Love waves the domain of quasilinearity is more limited (±4 per cent),

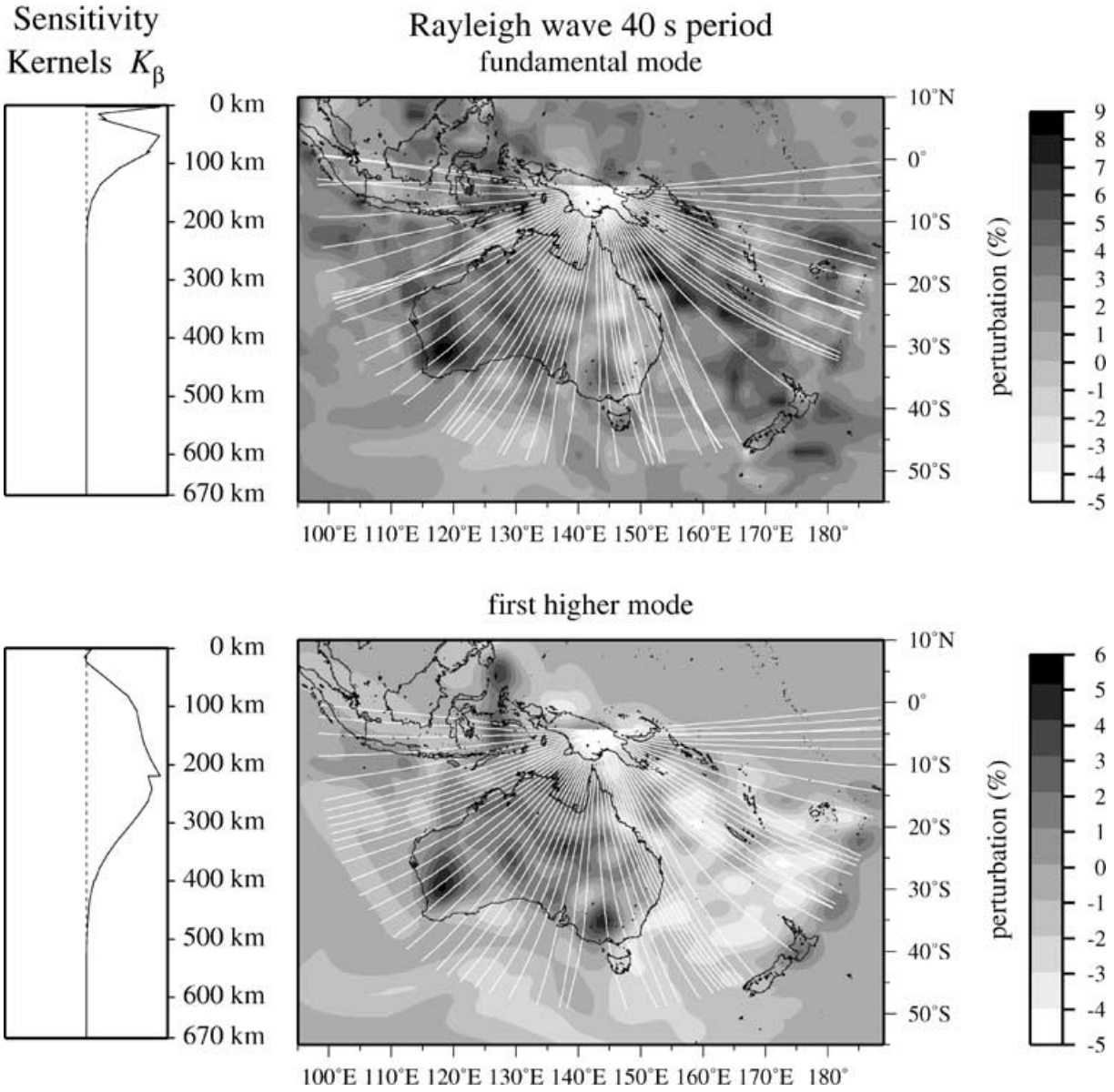

Figure 1. Illustrations of ray tracing for Rayleigh waves through the phase speed distribution derived from the shear wave speed model of Debayle & Kennett (2000a) for the Australian region. A uniform spray of rays is initiated from a source in New Guinea for both the fundamental and first higher mode at 40 s period and tracked across the phase speed maps for the two modes. At the left the sensitivity of the mode contributions to velocity structure with depth are indicated through the partial derivatives with respect to shear wave speed. To the right the keys indicate the level of phase speed perturbation from reference speeds of 3.93 km s^{-1} for the fundamental mode and 4.87 km s^{-1} for the first higher mode.

because of the strong overlap of the fundamental and higher mode contributions.

As the frequency of the surface waves is increased the influence of wave speed gradients become more marked. Gradients perpendicular to the propagation path lead to deviations of the propagation path from the great circle (Fig. 1) and gradients along the path tend to induce coupling between modes. These effects limit the range of frequencies over which path average approximations can be effective. The fundamental modes are strongly influenced by shallow structure and suffer substantial path deviations at higher frequencies. Mode-coupling is most important for the higher modes (Marquering *et al.* 1996). The influence of mode coupling can be restricted by suitable choice of the frequency window employed (Kennett 1995).

2.3 An alternative viewpoint

Rather than rely on perturbation methods we can seek a 1-D model $\beta'(z)$ such that for a set of modes

$$\phi_j(\omega) = p'_j(\omega)X, \tag{14}$$

over the frequency range of interest. We can then use $\beta'(z)$ as a representation of the multimode dispersion. This forms the basis of the fully non-linear inversion procedure for the waveforms of surface waves developed by Yoshizawa & Kennett (2002a), based on the use of the Neighbourhood Algorithm procedure of Sambridge (1999) for the exploration of parameter space.

The constraints on wave speed structure provided by the matching of waveforms are quite tight for any particular parametrization of

the wave speed profile. However, different styles of parametrization produce models with comparable fit to data but very different character. Nevertheless, the dispersion characteristics of the different successful models match very well.

If then we treat the models recovered from waveform inversion as a summary of multimode dispersion, we can work with somewhat less restrictive conditions than when we look for a path-averaged wave speed model. We still require the Earth to be smoothly varying so that we may employ the path-average approximation for phase, but significant deviations from the reference model can be accommodated. This viewpoint leads naturally to a three-stage inversion procedure to recover 3-D seismic structure, through the intermediary of multimode dispersion maps as a function of frequency.

It is still necessary to work with a band of frequencies chosen to ensure that frequencies are high enough that observations are made in the far-field of the source and so a simple representation can be used for the propagation terms, but not so high that mode coupling becomes important.

3 THREE-STEP INVERSION SCHEME

We propose a three-stage approach to the construction of 3-D models from surface wave data based on the development of multimode dispersion distributions as a function of frequency. This new style of surface wave tomography has the advantage of being able to accept information from a range of different sources and styles of interpretation and to integrate them in the model construction.

3.1 Multimode dispersion estimation

The first step in the construction of the model is to acquire path specific dispersion information for a number of modes crossing the region of interest. As uniform a path coverage as possible is needed to be able to get good resolution of lateral variations in dispersion at the second step.

Any style of estimate of phase dispersion may be used so that for long paths to global stations it can be appropriate to make direct dispersion estimates. Wherever possible such measurements should be extended to higher modes as in the mode stripping scheme of van Heijst & Woodhouse (1999), which depends on reasonable temporal separation between mode contributions.

Although it would be desirable to use direct extraction of phase contributions for different modes, at regional ranges the differences in group velocity are not sufficient to allow isolation of more than the fundamental mode, and even this is difficult for Love waves. We therefore need to employ indirect measurements of the phase properties. For regional ranges we can use waveform inversion for the surface wave seismograms as a means of obtaining summary 1-D velocity profiles for each path. Irrespective of the particular inversion scheme which has been used for the construction of the shear wave speed profile we can then use the 1-D model as a representation of the phase dispersion of the surface waves along the path (Yoshizawa & Kennett 2002a).

Because we are only using the 1-D models as a summary of multimode dispersion behaviour, we are able to use isotropic models to provide an independent description of the dispersion of Love waves and Rayleigh waves provided that anisotropic effects are small. The simplification of model descriptions has a number of significant advantages in increasing the flexibility of the tomographic process.

Previous analysis for Love and Rayleigh waves has focussed on the simultaneous inversion of the waveforms on the vertical and tangential components in terms of a transversely isotropic model with a vertical symmetry axis (see, e.g. Lévêque *et al.* 1998; Debayle & Kennett 2000b). The need for good recordings on both components is very restrictive, since it is necessary to avoid the nodal regions of both sets of radiation pattern.

In contrast by working with just the phase dispersion information summarized by a stratified model we are not restricted by the need to have both wavetypes well recorded. We are able to exploit all paths for which there are good recordings of Love waves and so markedly increase data coverage.

A useful addition to the dispersion information can also be extracted from horizontal component records in terms of the deviations of the arrival directions of surface waves from the great-circle, since such polarization information can be very significant for both studies of lateral heterogeneity and anisotropy (Laske & Masters 1996, 1998; Larson *et al.* 1998; Yoshizawa *et al.* 1999). At regional distances the differences in dispersion between Love and Rayleigh waves is such that both waves appear at the same times, and it is only the longer period portion of the Rayleigh wave train that is sufficiently separated for arrival angle estimates to be made. For longer paths the separation of the different components and modes is clearer and more use can be made of the polarization information.

3.2 Inversion for phase speed maps

Once the phase dispersion information has been assembled for a wide variety of paths the next step is to assemble phase dispersion maps as a function of frequency for the different mode branches. This process exploits the path-average property of the phase along each of the paths.

The first pass can be conducted as a linear inversion based on the assumption that the wave paths follow the great-circle, in which case each of the dispersion curves for a path can be regarded as a set of linear averaged constraints on the phase speed distribution across a sweep of frequencies. Such an inversion can be cellular or exploit a continuous representation as in the work of Montagner (1986).

This initial inversion then needs to be followed by iterative updates. We can trace rays directly in the phase speed domain and so the effects of the deviations of ray paths from the great-circle can be included in the improvement of the phase speed maps at each frequency.

Strong gradients in phase speed can produce significant ray path deviations particularly at higher frequencies. In Fig. 1 we show the patterns of propagation of Rayleigh waves from a source in New Guinea through phase speed distributions for 40 s waves derived from the shear wave speed model of Debayle & Kennett (2000a). We show both the fundamental and first higher modes and shoot a uniform distribution of rays from the source. The strong gradient in phase speed associated with the edge of the Australian shield near 140°E has the effect of introducing defocusing of the rays travelling close to north-south, and the gradients to the east also have a significant influence. The effects are more severe for the fundamental mode where the sensitivity is greatest for structure in the uppermost part of the mantle. There is a notable bunching of rays along the transition from continental to oceanic mantle in northwestern Australia. Even for the first higher mode, which samples the top 300 km of the mantle, there are perceptible deviations from the great-circle around the shield edge and in the Tasman Sea to the east. Two-point ray tracing shows that the deviations from the geodesic path rarely exceed 300 km. However, the focussing and defocusing effects evident in Fig. 1 have the effect of modulating the radiation

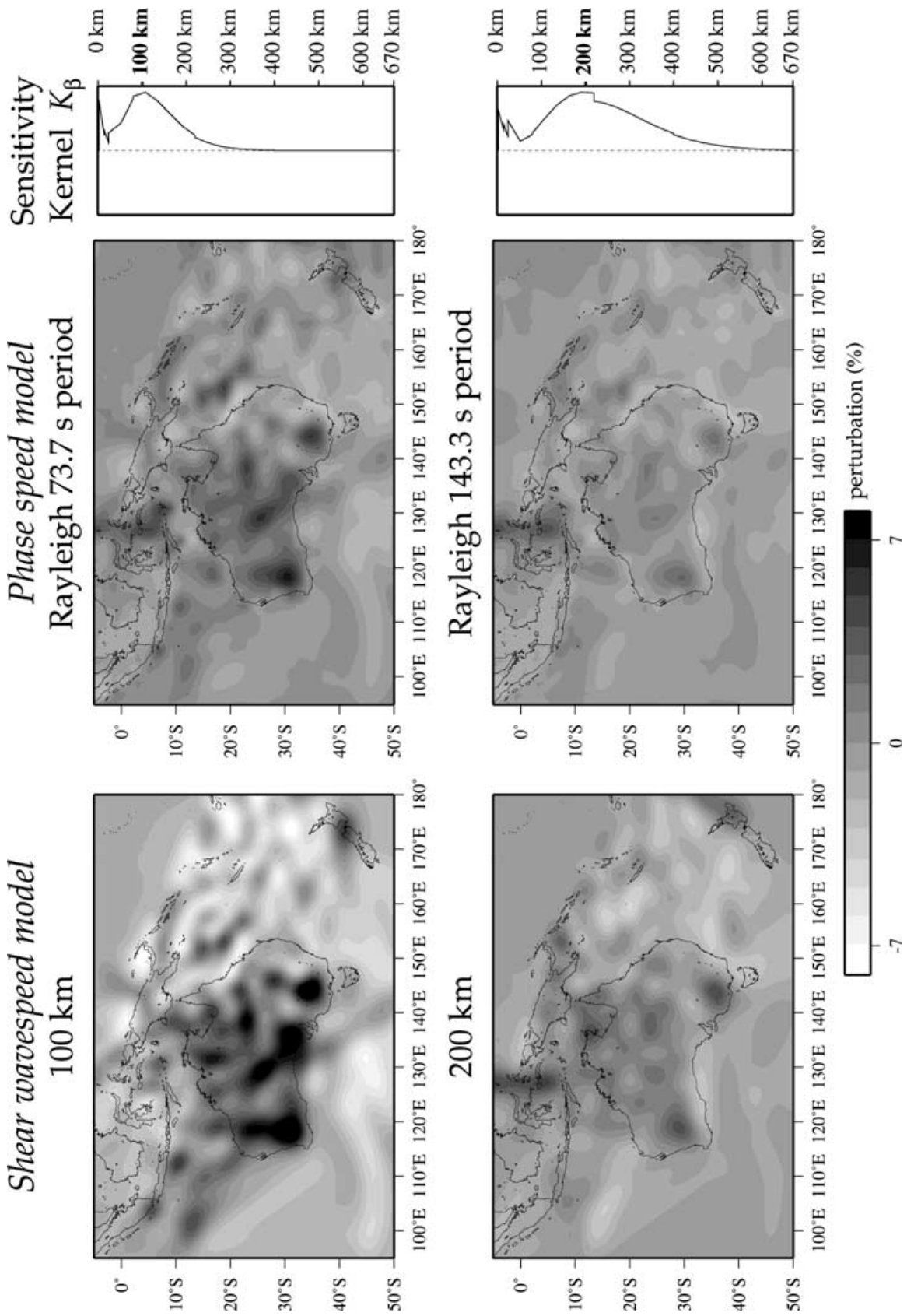

Figure 2. Comparison of map views of the shear wave speed model of Debayle & Kennett (2000a) for the Australian region with the phase speed maps for fundamental mode Rayleigh waves at periods where the sensitivity peaks at the same depths. The sensitivity of the mode contributions to velocity structure with depth are indicated through the partial derivatives with respect to shear wave speed at the right. The reference velocity for the wave speed variation is 4.40 km s^{-1} at 100 km and 4.43 km s^{-1} at 200 km, and for the phase speeds 4.01 km s^{-1} at 73.7 s and 4.26 km s^{-1} at 143.3 s period.

pattern imposed by the source and in extreme cases may mean that a waveform inversion is rejected on amplitude grounds.

In the phase speed domain we can not only include ray deviation but also make a direct allowance for the influence zone surrounding a wave path (Yoshizawa & Kennett 2002b), approximately one-third of the first Fresnel zone, which arises from the finite frequency of the surface waves. This zone has a typical half-width, transverse to the path, of about 100 km for the fundamental mode at 40 s period, and increases to close to 200 km at 100 s period. The effect of the influence zone is a natural smoothing out of short-wavelengths from the phase speed maps due to the healing of small perturbations in the wavefronts by diffraction processes.

Once the phase speed maps and phase dispersion measurements are mutually consistent, we can also include any available arrival-angle information and use an iterative improvement using ray tracing to match the full set of available data.

The patterns of crossing paths provide constraints on the angular variations in phase speed associated with possible anisotropy. We anticipate that the Rayleigh wave speed will display an angular variation characterized by terms dependent on azimuth θ through $\cos 2\theta$, $\sin 2\theta$, which can in principal be extracted with 5 crossing paths. For Love waves the dominant terms induced by slight anisotropy have a $\cos 4\theta$, $\sin 4\theta$ dependence and are more difficult to determine effectively.

As pointed out by Larson *et al.* (1998), rendition of even slightly anisotropic structure is best accomplished using anisotropic ray theory. The logical progression is therefore to develop the isotropic model, include anisotropy at first by a perturbation analysis and then finally undertake anisotropic ray tracing.

The use of phase-speed maps at a number of frequencies thus provides a working environment in which a wide range of different sources of information can be brought together for mutual benefit. We can for example make use of long-wavelength phase speed maps derived from global studies to provide the initial framework on which the more detailed information from regional paths can be superimposed. This also has the merit of including information from very long-period waves which are not well recorded in the data from portable broad-band instruments which form the bulk of many regional studies.

There is a close relation between the phase speed variations and the associated 3-D variations in wave speed. The phase speed maps reflect the velocity information as seen through a set of variable filters dictated by the character of the modal eigenfunctions. The interrelation is illustrated in Fig. 2 with map sections through the model of Debayle & Kennett (2000a) contrasted with the phase speed distribution for the fundamental mode at frequencies chosen to have maximum sensitivity at the same depths. These relations can be exploited in the final stage inversion for 3-D structure.

3.3 Inversion for wave speed structure

The final step of the inversion scheme exploits the localisation of phase-speed information with local inversions for 1-D shear wave speed profiles. We need to assemble the full set of multimode phase dispersion maps as a function of frequency and then use some form of cellular inversion to extract a 3-D model. Within each cell we combine the local information for each mode to construct a set of dispersion curves as a function of frequency including azimuthal effects and then undertake a stratified medium inversion for a local 1-D wave speed profile including anisotropy. The smoothing applied in the construction of the phase-speed maps, both to stabilise the inversion and also through the finite-frequency influence functions will mean a high degree of correlation between the dispersion properties in nearby cells, and hence of the wave speed profiles.

There may be merits in using an irregular cell system, e.g. through Delaunay triangulation (Sambridge *et al.* 1995), to allow for variations in the sampling by paths particularly on the edges of regions.

4 DISCUSSION

Although the 3-stage tomographic inversion procedure is less direct than methods such as partitioned waveform inversion, it provides a convenient means of studying regions with large contrasts in structure. By using the intermediary of phase speed maps as a function of frequency we can make allowances for finite frequency effects and undertake an iterative linearized inversion to account for the influence of strong heterogeneity via ray path deviation. It is also possible to include angle of incidence measurements of the polarization of fundamental mode Rayleigh waves in regional studies.

The three stage inversion allows the development of structure utilizing information from larger scale studies such as global models with the additional of regional information on phase dispersion obtained by any convenient means such as direct measurements or estimates of dispersion derived from 1-D models obtained by waveform inversion. Because the dispersion content is not dependent on the particular parametrization employed in the waveform inversion, 1-D models from different styles of waveform matching can be combined through their dispersion characteristics.

It is possible to use simple models for waveform inversion and use separate isotropic representations of Love and Rayleigh wave dispersion. This enables full coverage of Love and Rayleigh wave paths to be exploited and offers the potential of better resolution of anisotropic effects especially for Love waves.

The scheme we have described is designed to exploit the phase dispersion of surface waves, particularly through the influence on seismic waveforms. However there is also a valuable set of information on seismic structure available through group velocity studies (see, e.g. Ritzwoller & Levshin 1998). Hitherto the phase and group speed information has normally been treated separately because of the very different styles of analysis used. With the new emphasis on dispersion maps as a common vehicle for different types of phase based information we can envisage augmenting the third step in the tomographic inversion by undertaking a simultaneous inversion of phase and group velocity information for the localised cells (*cf.* Villaseñor *et al.* 2001).

If we work with complex slowness, we can include attenuation effects in the three-stage analysis and, in principle at least, begin to bring amplitude information to bear on the 3-D wave speed structure, including the influence of focusing and defocusing.

The present inversion scheme is based on neglect of mode coupling effects, but once we have a 3-D model we can test these assumptions by looking at coupling effects along individual paths (*cf.* Marquering *et al.* 1996) even though a full 3-D treatment (Kennett 1998) is currently too computationally demanding. We can envisage using the 3-D model to provide a basis for a perturbation treatment with mode-coupling to extend the analysis of the seismograms to higher frequencies and thereby improve the interpretation of the body wave information represented by the higher modes.

REFERENCES

Cara, M. & Lévêque, J.J., 1987. Waveform inversion using secondary observables, *Geophys. Res. Lett.,* **14,** 1046–1049.

Debayle, E. & Kennett, B.L.N., 2000a. The Australian upper-mantle: Structure and deformation inferred from surface waves, *J. geophys. Res.,* **105,** 25 243–25 450.

Debayle, E. & Kennett, B.L.N., 2000b. Anisotropy in the Australian upper mantle from Love and Rayleigh waveform inversion, *Earth planet. Sci. Lett.,* **184,** 339–351.

Hiyoshi, Y., 2001. Regional surface waveform inversion for Australian Paths, *PhD thesis,* Australian National University, Canberra.

Kennett, B.L.N., 1995. Approximations for surface-wave propagation in laterally varying media, *Geophys. J. Int.,* **122,** 470–478.

Kennett, B.L.N., 1998. Guided waves in 3-dimensional structures, *Geophys. J. Int.,* **133,** 155–174.

Larson, E.W.F., Tromp, J. & Ekström, G., 1998. Effects of slight anisotropy on surface waves, *Geophys. J. Int.,* **132,** 654–666.

Laske, G. & Masters, G., 1996. Constraints on global phase velocity maps by long-period polarization data, *J. geophys. Res.,* **101,** 16 059–16 075.

Laske, G. & Masters, G., 1998. Surface-wave polarization data and global anisotropic structure, *Geophys. J. Int.,* **132,** 508–520.

Lévêque, J.J., Debayle, E. & Maupin, V., 1998. Anisotropy in the Indian Ocean upper mantle from Rayleigh- and Love-waveform inversion, *Geophys. J. Int.,* **133,** 529–540.

Marquering, H., Snieder, R. & Nolet, G., 1996. Waveform inversions and the significance of surface-wave mode coupling, *Geophys. J. Int.,* **124,** 258–278.

Montagner, J.P., 1986. Regional three-dimensional structures using long-period surface waves, *Ann. Geophys.,* **4,** 283–294.

Nolet, G., 1990. Partitioned waveform inversion and two dimensional structure under the network of autonomously recording seismographs, *J. geophys. Res.,* **95,** 8499–8512.

Nolet, G., van Trier, J. & Huisman, R., 1986. A formalism for nonlinear inversion of seismic surface waves, *Geophys. Res. Lett.,* **13,** 26–29.

Ritzwoller, M.H. & Levshin, A.L., 1998. Eurasian surface wave tomography: Group velocities, *J. geophys. Res.,* **103,** 4839–4878.

Sambridge, M.S., 1999. Geophysical inversion with a neighbourhood algorithm—I. Searching a parameter space, *Geophys. J. Int.,* **138,** 479–494.

Sambridge, M.S., Braun, J. & McQueen, H., 1995. Geophysical parametrization and interpolation of irregular data using natural neighbours, *Geophys. J. Int.,* **122,** 837–857.

Simons, F.J., Zielhuis, A. & van der Hilst, R.D., 1999. The deep structure of the Australian continent from surface wave tomography, *Lithos,* **48,** 17–43.

van Heijst, H. & Woodhouse, J.H., 1999. Global high resolution phase velocity distributions of overtone and fundamental-mode surface waves determined by mode stripping, *Geophys. J. Int.,* **137,** 601–620.

Villaseñor, A., Ritzwoller, M.H., Levshin, A.L., Barmin, M.P., Engdahl, E.R., Spakman, W. & Trampert, J., 2001. Shear velocity structure of central Eurasia from inversion of surface wave velocities, *Phys. Earth planet. Inter.,* **123,** 169–184.

Woodhouse, J.H., 1974. Surface waves in a laterally varying layered structure, *Geophys. J. R. astr. Soc.,* **37,** 461–490.

Yoshizawa, K. & Kennett, B.L.N., 2002a. Nonlinear waveform inversion for surface waves with a neighbourhood algorithm—Application to multi-mode dispersion measurements, *Geophys. J. Int.,* **149,** 118–134.

Yoshizawa, K. & Kennett, B.L.N., 2002b. Determination of the influence zone for surface wave paths, *Geophys. J. Int.,* **149,** 441–455.

Yoshizawa, K., Yomogida, K. & Tsuboi, S., 1999. Resolving power of surface wave polarization data for higher-order heterogeneities, *Geophys. J. Int.,* **138,** 205–220.

Zielhuis, A. & Nolet, G., 1994. Shear-wave velocity variations in the upper mantle beneath central Europe, *Geophys. J. Int.,* **117,** 695–715.